Article

Cell Host & Microbe

Activation-Dependent Destruction of a Co-receptor by a *Pseudomonas syringae* Effector Dampens Plant Immunity

Graphical Abstract

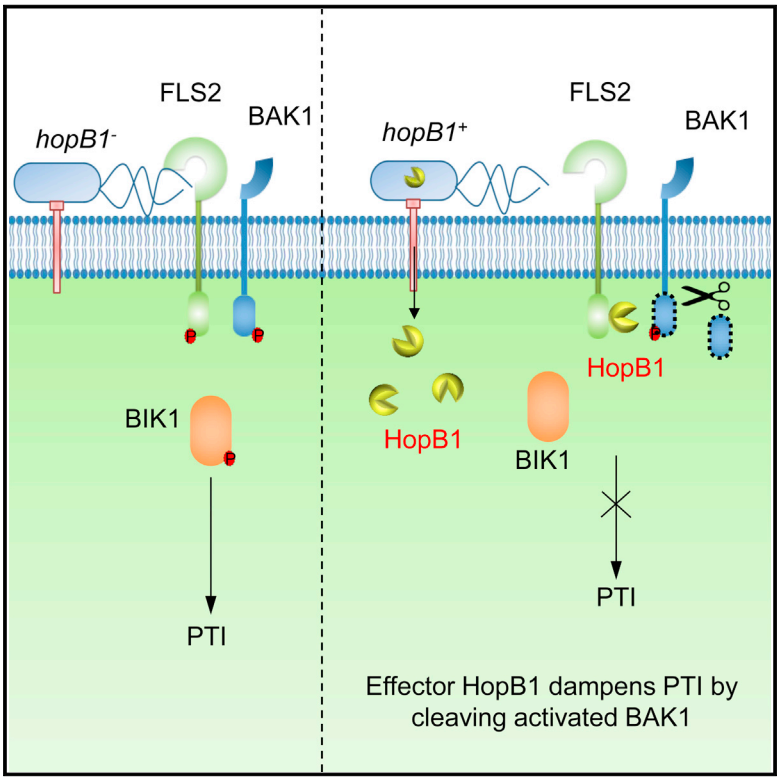

Highlights

- HopB1 enhances virulence, but not disease resistance, in *Arabidopsis*
- HopB1 cleaves immune co-receptor BAK1 to inhibit plant defenses
- HopB1-mediated cleavage requires an immune activation of BAK1
- A BAK1 mutant resistant to cleavage confers HopB1-insensitive immune responses

Authors

Lei Li, Panya Kim, Liping Yu, Gaihong Cai, She Chen, James R. Alfano, Jian-Min Zhou

Correspondence

lilei2011@genetics.ac.cn (L.L.), jmzhou@genetics.ac.cn (J.-M.Z.)

In Brief

The *Arabidopsis* BAK1 is a co-receptor required for the detection of pathogen molecules and subsequent immune activation, leading to increased disease resistance. Li et al. find that the *Pseudomonas* effector HopB1 is a protease that specifically degrades immune-activated BAK1, thus conferring increased virulence without overly perturbing the host plant.

Li et al., 2016, Cell Host & Microbe *20*, 504–514
October 12, 2016
http://dx.doi.org/10.1016/j.chom.2016.09.007

CellPress

Cell Host & Microbe
Article

Activation-Dependent Destruction of a Co-receptor by a *Pseudomonas syringae* Effector Dampens Plant Immunity

Lei Li,[1,5,*] Panya Kim,[2,5] Liping Yu,[1,5] Gaihong Cai,[3] She Chen,[3] James R. Alfano,[4] and Jian-Min Zhou[1,6,*]
[1]State Key Laboratory of Plant Genomics, Institute of Genetics and Developmental Biology, Chinese Academy of Sciences (CAS), Beijing 100101, China
[2]Center for Plant Science Innovation and School of Biological Sciences, University of Nebraska, Lincoln, NE 68588, USA
[3]National Institute of Biological Sciences, Beijing 102206, China
[4]Center for Plant Science Innovation and Department of Plant Pathology, University of Nebraska, Lincoln, NE 68588, USA
[5]Co-first author
[6]Lead contact
*Correspondence: lilei2011@genetics.ac.cn (L.L.), jmzhou@genetics.ac.cn (J.-M.Z.)
http://dx.doi.org/10.1016/j.chom.2016.09.007

SUMMARY

The *Arabidopsis* immune receptor FLS2 and co-receptor BAK1 perceive the bacterial flagellin epitope flg22 to activate plant immunity. To prevent this response, phytopathogenic bacteria deploy a repertoire of effector proteins to perturb immune signaling. However, the effector-induced perturbation is often sensed by the host, triggering another layer of immunity. We report that the *Pseudomonas syringae* effector HopB1 acts as a protease to cleave immune-activated BAK1. Prior to activation, HopB1 constitutively interacts with FLS2. Upon activation by flg22, BAK1 is recruited to the FLS2-HopB1 complex and is phosphorylated at Thr455. HopB1 then specifically cleaves BAK1 between Arg297 and Gly298 to inhibit FLS2 signaling. Although perturbation of BAK1 is known to trigger increased immune responses in plants, the HopB1-mediated cleavage of BAK1 leads to enhanced virulence, but not disease resistance. This study thus reveals a virulence strategy by which a pathogen effector attacks the plant immune system with minimal host perturbation.

INTRODUCTION

Plants and phytopathogens are engaged in a perpetual evolutionary battle. Plants employ multiple mechanisms to detect potential pathogens and activate innate immunity (Dodds and Rathjen, 2010; Jones and Dangl, 2006). Plasma membrane-localized pattern recognition receptors (PRRs), which are functionally analogous to animal Toll-like receptors, recognize conserved microbial molecules referred to as pathogen/microbe-associated molecular patterns (PAMPs/MAMPs), thereby inducing defense response (Boller and Felix, 2009; Macho and Zipfel, 2014). Pattern-triggered immunity (PTI) constitutes a first layer of plant immunity, to prevent parasitism of a broad range of potential phytopathogens. Phytopathogens can deliver a plethora of effector proteins into host cells to promote parasitism (Dou and Zhou, 2012; Macho and Zipfel, 2015). To counter pathogen effectors, plants have evolved a second layer of immunity consisting of intracellular NOD-like receptors (NLRs) that recognize specific effector proteins, leading to effector-triggered immunity (ETI; Cui et al., 2015; Spoel and Dong, 2012). The fact that effectors can be a double-edged sword represents a major dilemma in the adaptation of phytopathogens to their host plants (Alfano and Collmer, 2004).

Gram-negative pathogenic bacteria utilize type III protein secretion systems (T3SSs) to inject effectors (T3Es) into host cells. For instance, the model bacterial pathogen *Pseudomonas syringae* pv. *tomato* (*Pto*) DC3000 injects more than 30 T3E proteins into plant cells. Many T3Es encode enzymes such as phosphothreonine lyase, ADP-ribosyltransferase, uridylyltransferase, E3 ligase, acetyltransferase, tyrosine phosphatase, and cysteine protease (Feng and Zhou, 2012; Kazan and Lyons, 2014; Macho and Zipfel, 2015). While T3Es target specific host proteins to enhance bacterial virulence, the modification of host proteins often allows the plant to sense the pathogen and trigger ETI when one of the modified host proteins is guarded by a cognate NLR, thereby "betraying" the pathogen (Cui et al., 2015; Khan et al., 2016).

FLS2, a well-known PRR, recognizes a 22 amino acid N-terminal epitope (flg22) of bacterial flagellin. Perception of flg22 induces heterodimerization of FLS2 with its co-receptor BAK1 and activates the FLS2 receptor complex (Chinchilla et al., 2007; Heese et al., 2007; Sun et al., 2013). In addition to FLS2 signaling, BAK1 also serves as a co-receptor for additional PRRs including EFR, PEPRs (Roux et al., 2011), and likely RLP30 (Zhang et al., 2013) and RLP23 (Albert et al., 2015). Furthermore, the receptor-like cytoplasmic kinase (RLCK) BIK1 and its paralogs are part of multiple PRR complexes that regulate immune responses by phosphorylating downstream components (Kadota et al., 2014; Li et al., 2014; Lu et al., 2010; Zhang et al., 2010). A number of T3Es have been shown to enhance virulence by targeting PTI signaling pathways (Feng and Zhou, 2012; Xin and He, 2013). Notably, *Pto* T3Es AvrPto, AvrPtoB, AvrPphB, and HopAO1 directly target components of PRR complexes to block PTI (Gimenez-Ibanez et al., 2009; Göhre et al., 2008; Macho et al., 2014; Xiang et al., 2008; Zhang et al.,

2010). Other *Pto* effectors, such as HopU1, HopM1, HopAI1, and HopF2, target downstream immune components to interfere with RNA metabolism (Fu et al., 2007; Nicaise et al., 2013), vesicle trafficking (Nomura et al., 2006; Lozano-Durán et al., 2014), and MAP kinase activation (Wang et al., 2010; Zhang et al., 2007). Not surprisingly, plants have evolved mechanisms to sense the perturbation of the PTI pathway by effectors. For example, both the *Pseudomonas* T3E AvrPphB and the *Xanthomonas* T3E AvrAC target BIK1 for virulence, but plants have evolved BIK1 paralogs PBS1 and PBL2 to recognize AvrPphB and AvrAC, respectively, and activate NLR-mediated ETI (Feng et al., 2012; Shao et al., 2003; Wang et al., 2015; Zhang et al., 2010). Likewise, the *Pto* T3Es AvrPto and AvrPtoB target the PRR complex to promote virulence, but plants have evolved the Pto kinase to sense these effectors by mimicking the virulence target (Ntoukakis et al., 2014; Zhou and Chai, 2008). The *Ralstonia* T3E PopP2 acetylates WRKY transcription factors to inhibit transcription of plant immune response genes, but the NLR protein RRS1 has integrated a WRKY domain to sense PopP2-induced acetylation and activate ETI (Le Roux et al., 2015; Sarris et al., 2015). Furthermore, genetic and microbial perturbation of BAK1 results in heightened immune responses in *Arabidopsis* (Dominguez-Ferreras et al., 2015; He et al., 2007; Yamada et al., 2016). Although it is not clear whether NLR proteins are involved, the existing evidence indicates that plants have evolved a mechanism to sense effectors that target BAK1 (Yamada et al., 2016; Tang and Zhou, 2016). It remains unclear whether and how bacteria have evolved PTI-inhibiting T3Es that evade recognition by the plants.

Here we show that the *Pto* T3E protein HopB1 is an unconventional serine protease that does not match the peptidase database MEROPS (http://merops.sanger.ac.uk; Rawlings et al., 2014). HopB1 specifically cleaves BAK1 between Arg297 and Gly298 to enhance *Pto* virulence. Unlike previously reported T3E proteases, HopB1 does not cleave its substrate until it is activated upon flg22 perception. Although HopB1 disrupts BAK1, it does not trigger plant disease resistance, suggesting that the specific cleavage of activated BAK1 has allowed HopB1 to evade host recognition.

RESULTS

HopB1 Inhibits Plant Immunity

We previously identified a number of *Pto* T3Es that inhibit flg22-induced transcription of a basal resistance gene, *NHO1* (Li et al., 2005). In this study, we investigated additional *Pto* T3Es for their ability to inhibit the flg22-responsive reporter gene *FRK1*. The *FRK1::LUC* induction in *Arabidopsis* protoplasts was strongly inhibited by HopAI1, a positive control, and several previously uncharacterized T3Es, including HopB1 (Figures S1A and S1B, available online), which is the focus of this study.

We next examined *FRK1::LUC* induction in protoplasts upon different PAMP treatments. HopB1 completely blocked flg22- and elf18-triggered *FRK1::LUC* expression, but did not appear to significantly inhibit chitin-induced *FRK1* expression (Figure 1A). Transgenic plants expressing HopB1-FLAG under the control of an estradiol-inducible promoter were generated to test whether HopB1 impedes resistance to *P. syringae* bacteria. Two independent *hopB1* transgenic lines supported 5- to 7-fold more bacterial growth than did wild-type plants when spray-inoculated with the nonpathogenic *Pto hrcC*$^{-}$ strain (Figure 1B), which is deficient in the T3SS and induces only PTI in plants. The growth of wild-type *Pto* on the *hopB1* transgenic lines was similar to growth on the wild-type plants when spray-inoculated, a result consistent with the notion that the *hopB1* transgene offers partial bacterial growth benefit compared to that provided by the full complement of *Pto* T3Es (Figure 1B). These results indicated that HopB1 can significantly compromise PTI.

To determine whether HopB1 enhances the virulence of *Pto*, we generated knockout mutants by unmarked mutagenesis using FLP recombinase. The *Pto* Δ*hopB1* mutant showed only a minor reduction in bacterial growth in *Arabidopsis* (Figure 1C). Because T3Es often act together for robust inhibition of PTI, we reasoned that the virulence function of *hopB1* might be masked by other PTI-inhibiting effectors. We therefore generated double- and triple-knockout mutants of *hopB1* in combination with mutants of *avrPto* and *avrPtoB*, which are major virulence contributors in *Pto* (He et al., 2006; Kvitko et al., 2009). Indeed, the Δ*avrPtoB hopB1* double mutant showed significant in planta bacterial growth reduction compared with Δ*avrPtoB* single mutant bacteria (Figure 1C). In addition, introduction of wild-type *hopB1* into the Δ*avrPtoB hopB1* double mutant restored bacterial growth in planta to the level of the Δ*avrPtoB*-containing empty vector pML123 (Figure 1D). These results demonstrate that on *Arabidopsis* plants, *hopB1* indeed contributes to virulence, at least in a *Pto* strain lacking *avrPtoB*.

HopB1 Targets an Immune Receptor Complex and Inhibits Early PTI Responses

To explore biochemical function and the host target by which HopB1 inhibits the PTI, we systematically analyzed early molecular events of PTI. The flg22-triggered reactive oxygen species (ROS) production, an early PTI response, was reduced to 25%–45% in *hopB1* transgenic lines compared to the wild-type control (Figure 2A). Expression of HopB1-FLAG in transgenic plants also significantly suppressed flg22-induced MAP kinase phosphorylation (Figure S2A). However, unlike the control T3E HopAI1, which specifically targets MAPKs to inhibit *FRK1* expression (Zhang et al., 2007), HopB1 did not inhibit *FRK1* expression activated by the constitutively active forms of MKK5 (MKK5^{DD}) and MEKK1 (ΔMEKK1; Figure S2B), indicating that HopB1 targets upstream of the MAP kinase cascade.

Flg22-induced BIK1 phosphorylation occurs immediately following activation of the FLS2-BAK1 receptor complex (Zhang et al., 2010). HopB1-FLAG, expressed in *Arabidopsis* protoplasts, inhibited the flg22-induced mobility shift of BIK1-HA on SDS-PAGE (Figure 2B), indicating an inhibition of BIK1 phosphorylation and suggesting that HopB1 directly targets the FLS2 receptor complex. In vitro GST pull-down assays indicated HopB1 can interact with the FLS2 kinase domain (FLS2KD), but not with the BAK1 kinase domain (BAK1KD) or BIK1 (Figure 2C). Co-immunoprecipitation assays (coIP) showed that HopB1 constitutively associated with FLS2, regardless of the presence or absence of flg22 (Figure 2D). Split-luciferase complementation assays in *Nicotiana benthamiana* also indicated that HopB1 can interact with FLS2, but not BAK1 or BIK1 (Figures 2E, S2C, and S2D).

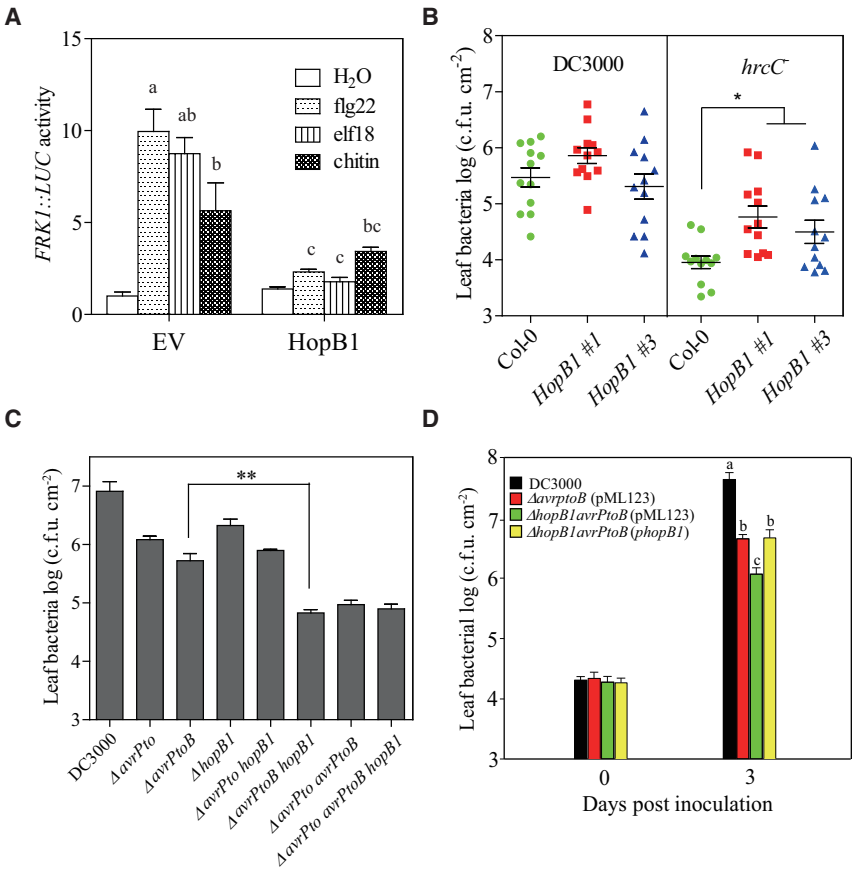

Figure 1. HopB1 Inhibits PAMP-Induced Immunity and Contributes to Bacterial Virulence

(A) HopB1 inhibits PAMP-induced *FRK1* expression in *Arabidopsis* protoplasts. *FRK1::LUC* activity was determined 3 hr after treatment with 1 μM flg22, 1 μM elf18, or 200 μg/mL chitin (data are represented as mean ± SEM; different letters indicate significant difference; Student's t test, $p \leq 0.05$; $n \geq 3$; two biological repeats).

(B) Expression of HopB1-FLAG contributes to the growth of *Pto hrcC*⁻ bacteria. Wild-type (Col-0) and *hopB1* transgenic plants were induced with 50 μM estradiol, after 24 hr they were sprayed with the indicated bacteria, and the bacterial populations were determined 4 days post-inoculation (data are represented as mean ± SEM; asterisk (*) indicates significant difference; $^*p \leq 0.05$, Student's t test; $n \geq 8$; two biological repeats).

(C) *hopB1* promotes *Pto* virulence on *Arabidopsis* plants. The indicated *Pto* mutant bacterial strains were infiltrated into *Arabidopsis* leaves, and the bacterial population was determined 3 days post-inoculation (data are represented as mean ± SEM; double asterisk (**) indicates significant difference; $^{**}p \leq 0.01$, Student's t test; $n \geq 6$; three biological repeats).

(D) *hopB1* is essential for virulence function of *Pto* on *Arabidopsis*. Empty vector (pML123) or *hopB1* containing construct under its native promoter (*phopB1*) was transformed into Δ*avrPtoB* or Δ*avrPtoB hopB1* strains. The indicated bacterial strains were infiltrated into *Arabidopsis* leaves, and the bacterial growth was determined (data are represented as mean ± SEM; different letters indicate significant difference; $p \leq 0.05$, Student's t test; $n \geq 4$; three biological repeats).

See also Figure S1.

HopB1 Induces flg22-Dependent Cleavage of BAK1

We next sought to determine whether HopB1 impacts the accumulation of FLS2 and BAK1 by co-expressing FLS2-FLAG and HopB1-FLAG in protoplasts. In the absence of flg22 treatment, FLS2-FLAG and the endogenous BAK1 accumulated normally in the presence of HopB1 (Figure S3A). Surprisingly, a treatment of flg22 for 10 min led to severe reduction of BAK1, but not FLS2-FLAG, accumulation in protoplasts expressing HopB1, but not AvrPto (Figure S3A). Further analysis indicated that this flg22-triggered BAK1 reduction occurred within 2 min after treatment, and BAK1 further diminished over the course of 30 min (Figure 3A).

To test whether HopB1 directly degrades BAK1, we co-expressed GST-HopB1 and the His-tagged BAK1 kinase domain (BAK1KD-His) in *E.coli*. Interestingly, a cleaved product ~6 kD smaller than BAK1KD-His was produced in the presence of GST-HopB1, but not GST (Figure 3B). Incubation of affinity-purified BAK1KD-His with an increasing amount of purified GST-HopB1 resulted in an increasing amount of BAK1KD-His cleavage product (Figure S3B), demonstrating that HopB1 is indeed capable of cleaving BAK1. However, this cleavage was less pronounced than the flg22-induced BAK1 reduction in protoplasts expressing HopB1.

Re-examination of BAK1 protein in protoplasts revealed a 35 kD product of BAK1 concomitant with the reduction of the full-length BAK1 protein only when both HopB1 and flg22 were present (Figure 3C). Together, these results indicate that HopB1 is an endo-peptidase that cleaves BAK1 in an flg22-dependent manner.

HopB1 Cleaves BAK1 in the P Loop between Arg297 and Gly298

In order to identify cleavage sites, the cleavage product of BAK1KD was reacted with acetic anhydride, which acetylates N-terminal and lysine residues of proteins. The modified product was subject to tandem mass spectrum (MS) analysis. All BAK1 peptides starting at Gly298 were N-terminal acetyl modified (Figure 4A), suggesting that Gly298 is located in the N terminus of the product. Furthermore, the peptides detected in MS covered the majority of the BAK1KD (Figure S4A; Table S2), validating the reliability of MS results. To further confirm that the cleavage indeed occurred between Arg297 and Gly298, we substituted the two residues with Ala. $BAK1KD^{R297A}$ and $BAK1KD^{G298A}$ were completely resistant to cleavage by HopB1 (Figure 4B). An Arg297Lys substitution also significantly reduced BAK1 cleavage (Figure 4B), indicating that Arg297 is essential for HopB1 recognition. In contrast, Ala substitutions of Arg280, Glu281, Arg307, and Leu308, which showed no or incomplete N-terminal acetylation in MS results, had no effect on cleavage by HopB1 (Figure S4B). The aforementioned results demonstrate that HopB1 specifically cleaves BAK1 between Arg297 and Gly298.

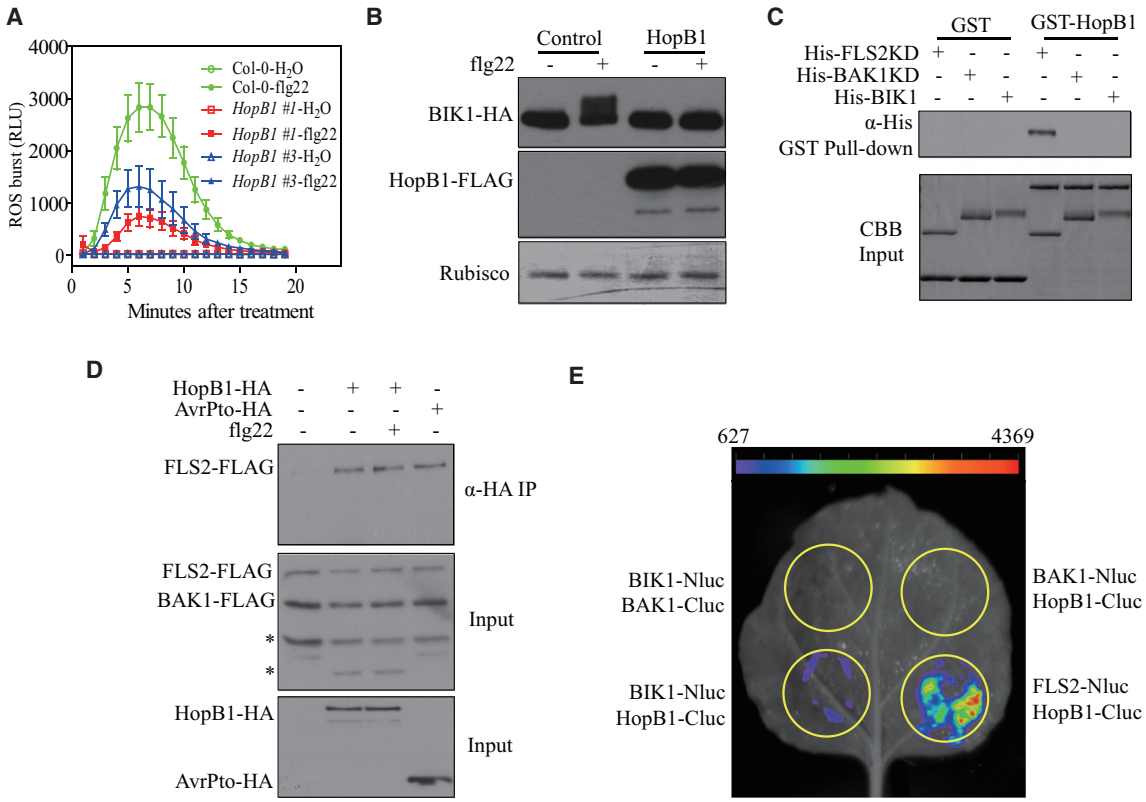

Figure 2. HopB1 Inhibits Early PTI Signaling Events by Interacting with FLS2

(A) HopB1 inhibits flg22-induced oxidative burst. Wild-type (Col-0) and transgenic plants expressing HopB1-FLAG were pretreated with 50 μM estradiol for 24 hr. Production of H_2O_2 was determined in two T2 independent transgenic lines.

(B) HopB1 inhibits flg22-induced BIK1-HA phosphorylation in *Arabidopsis* protoplasts. An HA-tagged BIK1 was co-expressed with HopB1-FLAG in wild-type (Col-0) protoplasts. Proteins were analyzed upon stimulation with 1 μM flg22 for 10 min. The experiments were repeated three times with similar results.

(C) HopB1 interacts with FLS2KD in vitro. GST-tagged HopB1 and His-tagged FLS2 kinase domain (FLS2KD), BAK1 kinase domain (BAK1KD), or BIK1 recombinant proteins were affinity purified, and the interaction was detected by GST pull-down assay. CBB, Coomassie brilliant blue staining.

(D) HopB1 interacts with FLS2 in vivo. HA-tagged HopB1 or AvrPto and FLAG-tagged FLS2 and BAK1 were co-expressed in wild-type *Arabidopsis* protoplasts. CoIP assay was performed using an anti-HA antibody to determine the interaction. Asterisk indicates truncated FLAG-tagged BAK1 proteins induced by HopB1 or in vivo proteolytic cleavage.

(E) HopB1 interacts with FLS2 in *Nicotiana benthamiana*. The *Agrobacterium* carrying the indicated constructs were infiltrated into *Nicotiana benthamiana* leaves, and luciferase complementation imaging assays were performed.

See also Figure S2.

BAK1 belongs to the SERK family, consisting of five members with redundant function (Roux et al., 2011). In vitro cleavage assays showed that HopB1 cleaved the kinase domain of all SERK members except for SERK5 (Figure S4C). A sequence alignment showed that while the other four members all contained the conserved cleavage sites, SERK5 contained an Arg-to-Lys mutation in this site (Figure S4D), explaining the lack of HopB1 recognition.

BAK1 and BKK1 Are Virulence Targets for HopB1

To determine whether SERK members are required for the virulence function of *hopB1*, we inoculated *bak1–5/bkk1* double-mutant plants with various *Pto* mutant strains. Unlike *bak1–4/bkk1*, which displays constitutive immune responses, *bak1–5/bkk1* is normal in the absence of PAMP stimulation (Schwessinger et al., 2011). *bak1–5* acts as a dominant-negative mutation that specifically impedes immune function of SERK members (Schwessinger et al., 2011). While the *Pto* Δ*avrPtoB* strain grew significantly more than the *Pto* Δ*avrPtoB hopB1* strain on wild-type plants, the two strains grew similarly on *bak1–5/bkk1* double mutant (Figure 4C), demonstrating that BAK1, BKK1, and likely other SERK members are virulence targets of HopB1.

We generated transgenic plants in *bak1–4* background expressing various forms of BAK1 under the control of a native promoter. In contrast to plants expressing wild-type BAK1 or $BAK1^{R297A}$, plants expressing $BAK1^{G298A}$ were completely abolished in flg22-triggered H_2O_2 production (Figures S4E and S4F), indicating that Gly298 is required for BAK1 function. Gly298 residue is located in the P loop of the kinase domain, suggesting that $BAK1KD^{G298A}$ may be defective in kinase activity. Indeed, autophosphorylation of $BAK1KD^{G298A}$ was significantly reduced compared to wild-type BAK1KD (Figure S4G). Consistent with the normal immune function of $BAK1^{R297A}$ in transgenic plants, $BAK1KD^{R297A}$ showed normal autophosphorylation (Figure S4G).

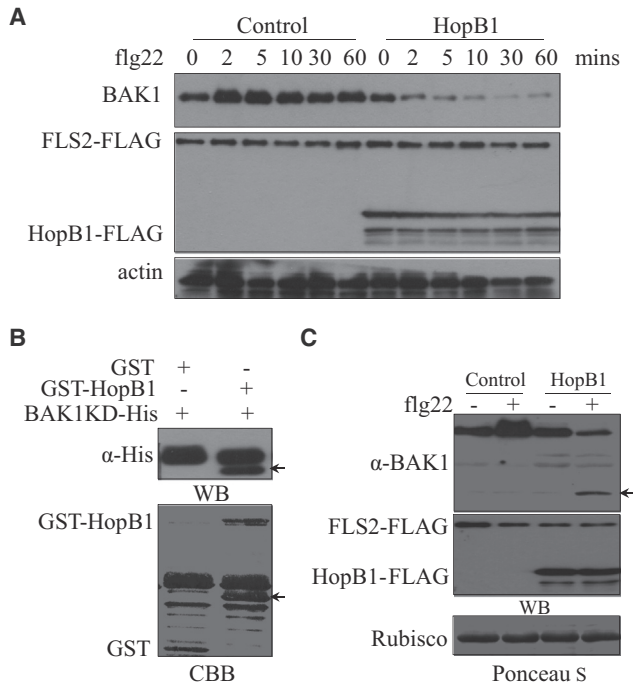

Figure 3. HopB1 Induces Cleavage of BAK1

(A) HopB1 induces degradation of endogenous BAK1 in an flg22-dependent manner. FLAG-tagged HopB1 and FLS2 were transiently expressed in *Arabidopsis* protoplasts. Upon treatment with 1 μM flg22 for the indicated times, total protein was extracted and immunoblots were performed using antibodies against FLAG, BAK1, and actin.

(B) The BAK1 kinase domain is cleaved by HopB1 in vitro. GST-tagged HopB1 and C-terminal His-tagged BAK1 kinase domain recombinant proteins were co-expressed in *E.coli*. Proteins were subject to immunoblots and Coomassie brilliant blue (CBB) staining. The arrow indicates BAK1 cleavage product.

(C) HopB1 cleaves endogenous BAK1 in *Arabidopsis* protoplasts. FLAG-tagged HopB1 and FLS2 were transiently expressed in protoplasts. Ten minutes after treatment with 1 μM flg22, total protein was extracted and analyzed by immunoblots using anti-FLAG and anti-BAK1 antibodies. The arrow indicates HopB1-induced BAK1 cleavage product. The experiments were repeated three times with similar results.

See also Figure S3.

The normal PTI function and resistance to HopB1 cleavage prompted us to test whether $BAK1^{R297A}$ confers immunity in a manner insensitive to HopB1. We expressed BIK1-HA in protoplasts derived from *bak1–4* lines complemented with wild-type *BAK1* or $BAK1^{R297A}$ transgenes and tested flg22-triggered BIK1 phosphorylation. Consistent with ROS assays, both transgenes restored flg22-induced BIK1 phosphorylation (Figure 4D). Co-expression with HopB1-FLAG inhibited the BIK1 phosphorylation in *BAK1* protoplasts, but had no effect in $BAK1^{R297A}$ protoplasts (Figure 4D), indicating that $BAK1^{R297A}$ can activate PTI signaling in the presence of HopB1. We further conducted virulence assays on these transgenic lines (*bak1–4* background), predicting that *hopB1* would confer reduced virulence on plants carrying $BAK1^{R297A}$. The *hopB1*-complemented *Pto* Δ*avrPtoB hopB1* strain grew more compared to *Pto* Δ*avrPtoB hopB1* on plants carrying the wild-type *BAK1* transgene (Figure S4H). In contrast, the two strains grew similarly on $BAK1^{R297A}$ transgenic plants. Although not statistically significant, plants carrying the wild-type *BAK1* transgene reproducibly supported greater growth of the *hopB1*-complemented *Pto* Δ*avrPtoB hopB1* bacteria than did the $BAK1^{R297A}$ transgenic plants in three independent experiments. The relatively weak resistance to *hopB1*-containing strain conferred by the $BAK1^{R297A}$ transgene is consistent with the notion that HopB1 targets redundant SERK family members (Figure S4C). Together, the results support that the $BAK1^{R297A}$ transgene confers *hopB1*-insensitive immunity.

HopB1 Cleavage of BAK1 Requires BAK1 Kinase Activity

The flg22-dependent cleavage suggests that HopB1 only recognizes the activated form of BAK1. Pretreatment of protoplasts with the kinase inhibitor K-252a significantly inhibited BAK1 cleavage by HopB1 (Figure 5A), suggesting that activation of FLS2 receptor complex is required for HopB1-mediated cleavage of BAK1.

To further test if BAK1 kinase activity is required for HopB1-mediated cleavage, recombinant proteins $BAK1KD^{K317E}$ and $BAK1KD^{D416N}$, which are mutated in the ATP-binding site and catalytic site, respectively, were co-expressed with GST-HopB1 in *E. coli*. Both mutant proteins were resistant to cleavage by HopB1 in vitro (Figure 5B). To further determine whether a specific phospho-site of BAK1KD is necessary for cleavage, we substituted known phospho-sites Thr449, Thr450, and Thr455 with Ala, and Tyr463 with Phe (Wang et al., 2008; Yan et al., 2012). Co-expression of the resulting mutant proteins with GST or GST-HopB1 in *E.coli* showed that only $BAK1KD^{T455A}$ was resistant to HopB1 cleavage (Figure 5B), indicating that BAK1 Thr455 phosphorylation is crucial for recognition by HopB1.

The tertiary structure of BAK1KD (PDB, 3TL8, and 3UIM) showed that the cleavage site (Arg297/Gly298) is located in the same surface as Thr455, but not Thr446, Thr449, Thr450, or Tyr463 (Figure 5C). The phosphorylation of Thr455 likely stabilizes the P loop, where Arg297 and Gly298 reside, thereby facilitating the recognition and/or cleavage by HopB1, which would explain the flg22-dependent action of HopB1. We cannot rule out the possibility that the HopB1 protease is activated upon phosphorylation by an active BAK1 kinase.

HopB1 Is a Serine Protease

According to catalytic residues, proteases are currently classified into four broad groups including serine protease, cysteine protease, aspartic acid protease, and metalloprotease. A BLAST search with the HopB1 primary sequence against MEROPS, which hosts an updated collection of all protease super-families (Rawlings et al., 2014), failed to identify similar sequences. Likewise, a sequence-structure bioinformatics analysis using HHpred software (Söding et al., 2005) failed to identify any domain of known biochemical function, indicating that HopB1 is a new family of proteases. To identify the properties of HopB1, we tested its sensitivity to a series of class-specific protease inhibitors. Cysteine protease inhibitor E-64, metalloprotease inhibitor EDTA, and aspartic acid protease inhibitor pepstatin did not affect HopB1-mediated cleavage (Figure 6A). However, serine protease inhibitors PMSF and AEBSF strongly inhibited BAK1KD cleavage by HopB1 (Figure 6A). Together, these results supported that HopB1 is a serine protease.

A

BAK1KD cleavage sites identified by LC-MS/MS analysis

Start - End	Partial Peptide Sequence	Variable modifications	Emergence rate of modification
281 - 297	R.ELQVASDNFSNKNILGR.G	Acetyl (K)	2/2
298 - 305	R.GGFGKVYK.G	Acetyl (K); Acetyl (N-term)	1/1;1/1
298 - 307	R.GGFGKVYKGR.L	Acetyl (K); Acetyl (N-term)	4/4;4/4
308 - 317	R.LADGTLVAVK.R	Acetyl (N-term)	1/2
308 - 318	R.LADGTLVAVKR.L	Acetyl (K); Acetyl (N-term)	15/16;13/16
312 - 318	G.TLVAVKR.L	Acetyl (K)	1/1

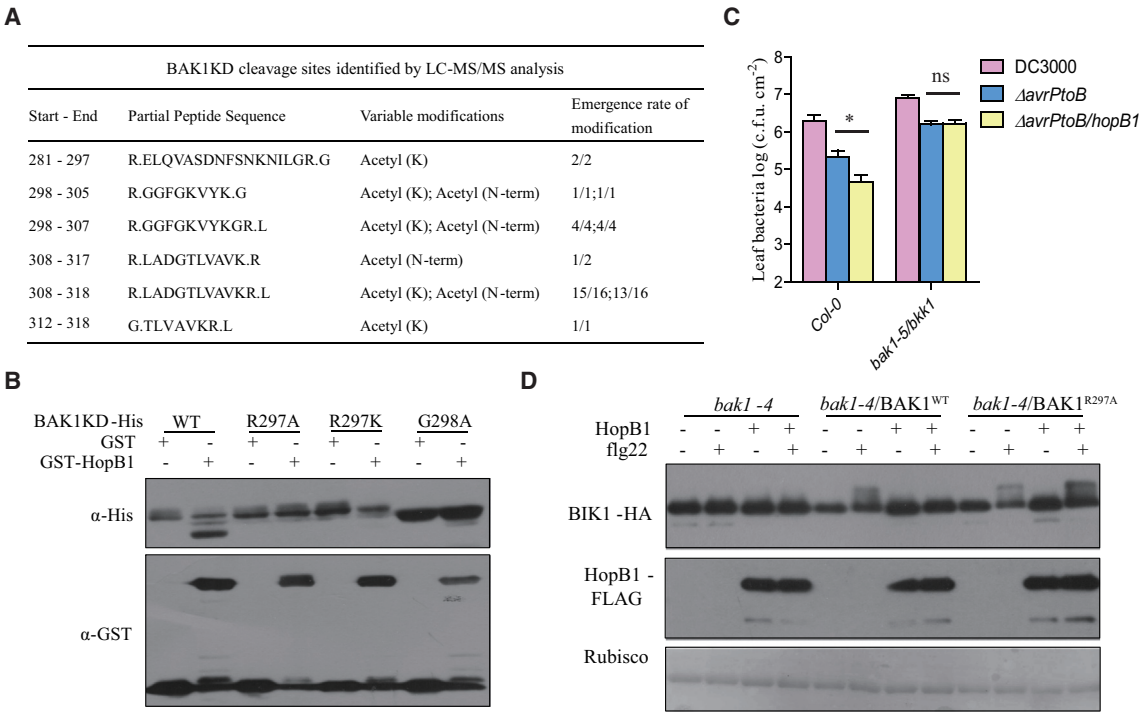

Figure 4. HopB1 Cleaves BAK1KD between Arg297 and Gly298, and BAK1/BKK1 Are Required for HopB1 Virulence in Plants

(A) HopB1 cleavage site in BAK1KD identified by using liquid chromatography-tandem mass spectrometry (LC-MS/MS) analysis. GST-HopB1 and BAK1KD-His were co-expressed in *E.coli*. His-tagged proteins were purified using an Ni-NTA column. The cleaved protein band was excised and reduced in 5% acetic anhydride for 1 hr to modify the N terminus with acetylation. Peptides with variable modifications were analyzed by LC-MS/MS. The emergence rate indicates the number of peptides with each modification to the total number of corresponding peptides identified in MS.

(B) Mutations of Arg297 and Gly298 inhibit BAK1KD cleavage by HopB1. GST-tagged HopB1 and indicated BAK1KD mutants were co-expressed in *E.coli*. Immunoblots were performed to analyze proteins. The experiments were performed two times with similar results.

(C) *hopB1* enhances *Pto* virulence on wild-type, but not *bak1–5/bkk1*, double-mutant plants. The bacteria strains were infiltrated into wild-type or *bak1–5/bkk1* mutant plants, and the number of bacterial growth was determined at 3 days after inoculation (data are represented as mean ± SEM; asterisk (*) indicates significant difference; *$p \leq 0.05$, Student's t test; $n \geq 8$; three biological repeats; ns, no significance).

(D) Cleavage of BAK1 is required for HopB1-mediated inhibition of BIK1 phosphorylation. HA-tagged BIK1 was co-expressed with HopB1-FLAG in protoplasts of genotype *bak1–4*, and *bak1–4* lines complemented with stable wild-type *BAK1* or $BAK1^{R297A}$. Upon stimulation with 1 μM flg22 for 10 min, proteins were detected by anti-HA and anti-FLAG immunoblots. The experiments were carried out three times with similar results.

See also Figure S4 and Table S2.

Deletion analyses were performed to determine HopB1 regions required for cleavage. An N-terminal truncated fragment of HopB1 ($HopB1^{123–466}$) was sufficient to cleave BAK1KD in vitro (Figure S5A). Since the serine residue acting as nucleophile in proteases can be replaced by a threonine residue (Rawlings and Barrett, 2013), we mutated all serine and threonine residues within $HopB1^{123–466}$ and found that only Thr370 was required for BAK1KD cleavage (Figures 6B and S5B). In addition to the Ser/Thr residue, the catalytic center of serine proteases often contains histidine and aspartate residues located near the N/C termini of β strands (Rawlings and Barrett, 2013). We thus used PSIPRED v3.3 to predict the secondary structure of HopB1 (Figure S5C). This identified His413, located near the C terminus of β3, and Asp435 and Asp436, located in the C terminus of β4, as candidate active sites (Figure S5C). Mutagenesis studies showed that $HopB1^{H413A}$, $HopB1^{D435A}$, and $HopB1^{D436A}$ were completely unable to cleave BAK1KD in vitro (Figure 6B). In contrast, $HopB1^{H427A}$ and $HopB1^{D446A}$ were fully capable of cleaving BAK1KD in vitro (Figure S5B), indicating that His413, Asp435, and Asp436 are specifically required for the protease activity. Furthermore, Thr370, His413, Asp435, and Asp436 are invariable residues among different *Pseudomonas* strains (Figure S5D). Together, the results suggest that Thr370, His413, Asp435, and Asp436 may collaboratively support the nucleophilic center to cleave the peptide bond.

To test the biological significance of the HopB1 protease activity, we co-expressed BIK1-HA and protease-dead HopB1 mutants in *Arabidopsis* protoplasts. While wild-type HopB1 completely inhibited flg22-induced BIK1-HA phosphorylation, $HopB1^{T370A}$, $HopB1^{H413A}$, $HopB1^{D435A}$, and $HopB1^{D436A}$ all failed to inhibit BIK1-HA phosphorylation (Figure S5E). In addition, reintroduction of wild-type *hopB1* into the *Pto* Δ*avrPtoB hopB1* double mutant restored bacterial growth in planta to the level found for the Δ*avrPtoB* strain. However, the protease-dead mutants $hopB1^{T370A}$, $hopB1^{H413A}$, $hopB1^{D435A}$, and $hopB1^{D436A}$ failed to complement the growth of the *Pto* Δ*avrPtoB hopB1* double mutant (Figure 6C). In transgenic plants expressing the protease-dead $HopB1^{H413A}$, $HopB1^{D435A}$, and $HopB1^{D436A}$ mutants, flg22-induced H_2O_2 production was restored to wild-type (Col-0) level (Figures 6D and S5F). Similar

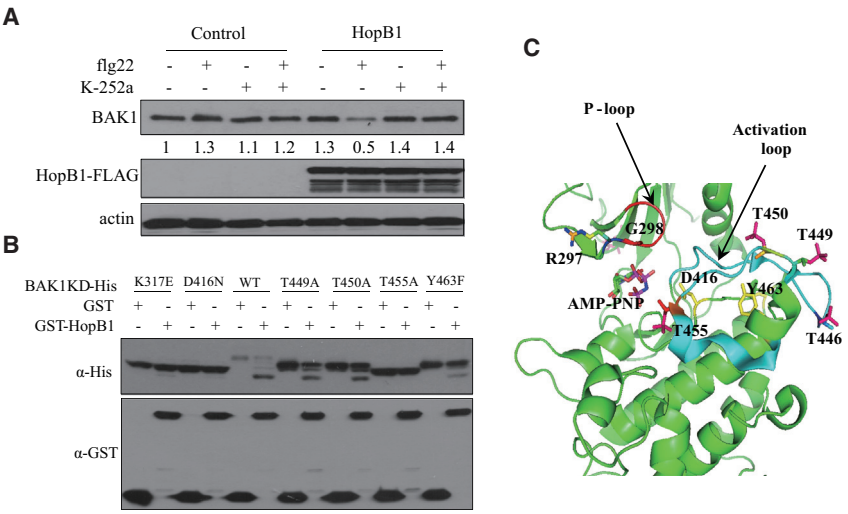

Figure 5. An Activated BAK1 Is Required for HopB1 Recognition and Cleavage

(A) Kinase inhibitor K-252a suppresses HopB1-mediated cleavage of endogenous BAK1. FLAG-tagged HopB1 was transiently expressed in wild-type *Arabidopsis* protoplasts. The protoplasts were treated with DMSO or K-252a for 1 hr prior to elicitation with 1 μM flg22, and immunoblots were performed to detect proteins using antibodies against FLAG, BAK1, and actin. Relative BAK1 band intensity was calculated by ImageJ software and indicated below. It is normalized to the corresponding actin band and relative to untreated sample.

(B) BAK1 kinase activity is required for HopB1-mediated cleavage of BAK1KD. GST-tagged HopB1 and indicated BAK1KD mutants were co-expressed in *E.coli*. Immunoblots were performed to analyze proteins.

(C) Structure of BAK1 kinase domain (PDB: 3TL8 and 3UIM). Cleavage site R297/Gly298 is located in the same surface of phospho-site T455. P loop and activation loop are labeled in red and cyan, respectively. Cleavage site R297/G298 and phospho-sites T446, T449, T450, T455, and Y463 are shown in stick form.

results were obtained when flg22-induced *FRK1* reporter gene expression was tested (Figure S5G). Taken together, these results demonstrate that protease activity is essential for HopB1-mediated inhibition of PTI and its contribution to bacterial virulence on *Arabidopsis* plants. Interestingly, the protease-dead HopB1 appeared to induce higher *FRK1* expression (Figure S5G), and wild-type HopB1 enhanced *FRK1* induction caused by constitutive activation of MAPK pathway (Figure S2B), indicating that overexpression of HopB1 may enhance plant immune responses through an unknown mechanism.

DISCUSSION

In this study, we showed that HopB1 inhibited early PTI events and compromised basal resistance to the *Pto hrcC*$^{-}$ mutant strain. Biochemical analyses demonstrated that HopB1 is a protease that cleaves the P loop of BAK1 only when the latter is activated upon flg22 perception. The flg22-induced activation of BAK1 is known to require the phosphorylation of Thr455, and we showed that this phosphorylation is required for cleavage by HopB1. We identified cleavage sites in BAK1 and amino acid residues in HopB1 required for the protease activity. Mutagenesis in BAK1 and HopB1 demonstrated that this specific proteolytic cleavage is essential for HopB1-mediated inhibition of PTI and virulence. This study uncovered a biochemical mechanism by which a T3E subverts plant immunity. HopB1 constitutively associates with FLS2. Upon flg22 perception, BAK1 is recruited to the FLS2 receptor complex and becomes phosphorylated. HopB1 cleaves the activated BAK1 to block downstream immune responses.

HopB1 contributes to virulence on *Arabidopsis* plants. The combination of *avrPtoB* and *hopB1* mutations resulted in poor bacterial growth in plants, indicating that *hopB1* contributes to *Pto* virulence. The Δ*avrPtoB hopB1* double-mutant strain showed a much greater reduction in virulence compared to either single mutant, a result consistent with previous findings that *Pto* T3Es act together to robustly inhibit host immunity (Cunnac et al., 2011; Kvitko et al., 2009).

Our analyses established that HopB1 as a protease specifically targets SERK kinases. Transgenic expression of HopB1 led to broad inhibition of early PTI signaling events and downstream responses in *Arabidopsis* plants and protoplasts. Expression of HopB1 led to degradation of BAK1 in flg22-induced protoplasts. Incubation of recombinant HopB1 cleaved the BAK1 kinase domain in vitro. HopB1 does not affect FLS2 and BIK1 accumulation, indicating that it is specific to BAK1. MS study showed that HopB1 cleaves BAK1 between Arg297 and Gly298. Mutations in these residues prevented cleavage. Similarly, all SERK family members carrying the cleavage site were cleaved by HopB1 in vitro, whereas SERK5, which carries a mutation in the cleavage site, was not. These residues are located in the P loop of the BAK1 kinase domain, and the cleavage is expected to render BAK1 nonfunctional, explaining the broad impact of HopB1 on PTI responses. Most importantly, the virulence function of *hopB1* is dependent on SERKs, as *hopB1* failed to enhance virulence on *bak1–5/bkk1* mutant plants, demonstrating that SERKs are virulence targets for HopB1. The study thus uncovers a molecular mechanism by which *Pto* T3E inhibits PTI for virulence.

HopB1 is an unusual protease that differs from all known proteases. All phytopathogenic T3E proteases identified to date belong to the cysteine protease family with a Cys-His-Asp catalytic triad to catalyze hydrolysis of peptide bonds. The *Pseudomonas* T3Es AvrPphB and AvrRpt2 are papain-like cysteine proteases (Axtell et al., 2003; Shao et al., 2002), whereas the *Xanthomonas* T3E XopD is a SUMO protease (Hotson et al., 2003; Kim et al., 2013). Unlike AvrPphB and AvrRpt2, HopB1 does not appear to require autoproteolytic processing for activation. HopB1 does not share the Cys-His-Asp catalytic triad and is insensitive to cysteine protease inhibitors. Instead, the serine

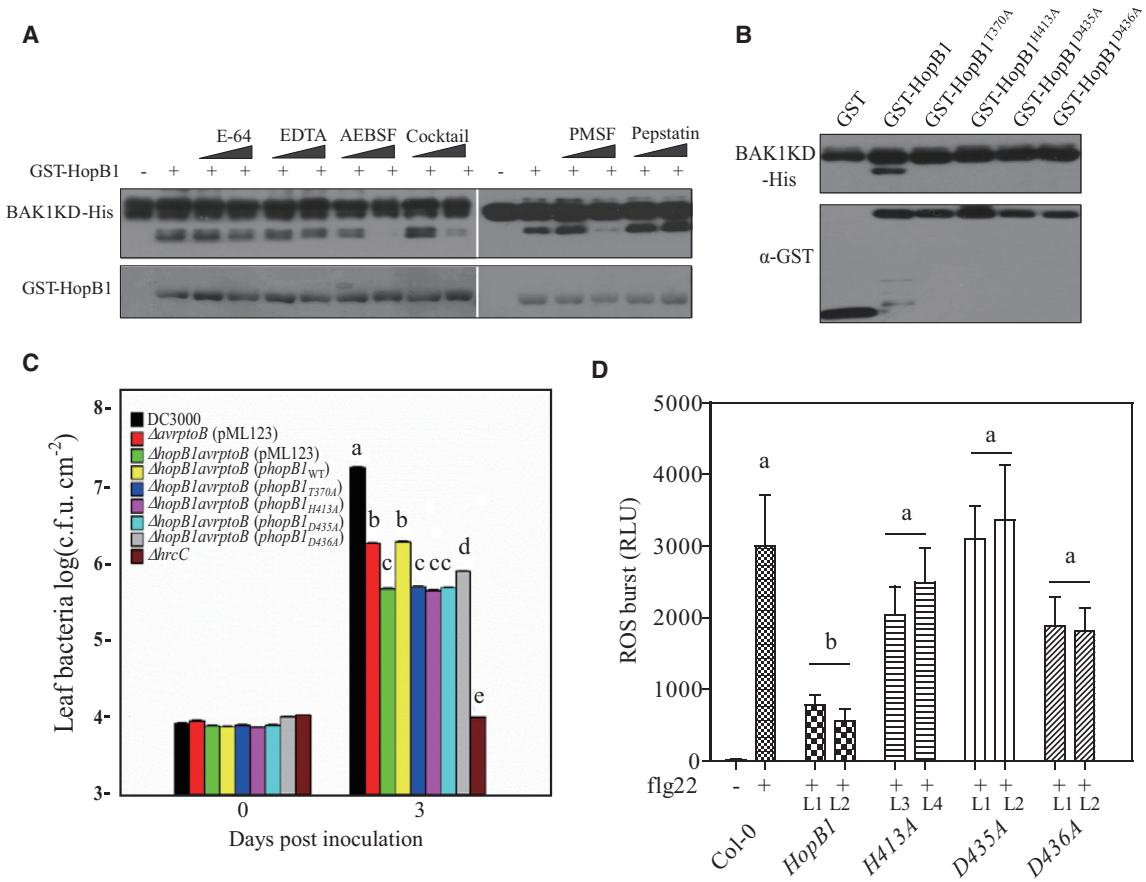

Figure 6. HopB1 Acts as a Protease to Inhibit Plant Immunity

(A) Serine protease inhibitors AEBSF and PMSF prevent BAK1KD cleavage by HopB1. His-tagged BAK1KD and GST-HopB1 recombinant proteins were affinity purified and incubated together in a tube at 25°C for 7 hr. BAK1KD-His and the cleavage product were detected using anti-His immunoblot. GST-HopB1 was stained by Coomassie brilliant blue (CBB). The protease inhibitor cocktail is a mixture containing AEBSF, Bestatin, E-64, Pepstatin, and EDTA.

(B) Residues of HopB1 required for BAK1KD cleavage. His-tagged BAK1KD and indicated GST-HopB1 mutants were co-expressed in *E.coli*, and total proteins were subjected to immunoblot analysis.

(C) Protease activity of HopB1 is essential for its virulence to *Pto* on *Arabidopsis*. The indicated *Pto* bacterial strains were infiltrated into *Arabidopsis* leaves, and the bacterial growth was determined (data are represented as mean ± SEM; different letters indicate significant difference; $p \leq 0.05$, Student's t test; $n \geq 4$; two biological repeats).

(D) HopB1 protease activity is required for its inhibition of flg22-induced H_2O_2 production in plants. Wild-type (Col-0) and transgenic plants expressing the indicated *HopB1* mutants were pretreated with estradiol for 24 hr. Production of H_2O_2 was determined upon stimulation with H_2O or 100 nM flg22 in two independent T2 lines (data are represented as mean ± SEM; different letters indicate significant difference; $p \leq 0.05$, Student's t test; $n \geq 8$; two biological repeats). See also Figure S5.

protease inhibitors PMSF and AEBSF specifically prevented BAK1KD cleavage by HopB1, indicating HopB1 is likely a serine protease. However, HopB1 primary sequence and secondary structure failed to show similarity with sequences in the peptidase database MEROPS (Rawlings et al., 2014). Serine proteases are members of one of the largest families, accounting for one-third of proteolytic enzymes. They typically possess a catalytic triad of Asp-His-Ser, with the serine residue existing in an oxyanion hole and serving as a nucleophilic amino acid to cleave the peptide bond (Hedstrom, 2002; Powers et al., 2002; Rawlings and Barrett, 2013). HopB1 does not appear to carry the typical serine protease catalytic triad. Among all Ser/Thr residues tested, Thr370 was the only one required for HopB1 protease activity. Given that sulfonyl fluorides may react with other hydroxyl amino acids except for serine (Narayanan and Jones, 2015), and that catalytic serine residue is replaced by threonine in several homologs of serine protease such as TSP50 and an artificial trypsin (Baird et al., 2006; Xu et al., 2007), Thr370 may be part of the catalytic center of the HopB1 protease. In addition, His413, Asp435, and Asp436, located near the C termini of β strands in the predicted secondary structure, are also required for HopB1 protease activity. These residues may provide nucleophilic groups for catalysis, although we cannot exclude the possibility that they are involved in protein folding. Future biochemical and structural studies will elucidate the organization of the catalytic center and mode of action of HopB1. Importantly, all residues required for HopB1 protease activity are also required for inhibition of PTI and bacterial virulence, further demonstrating that HopB1 uses a unique protease activity to assist *Pto* infection in plants.

As a common co-receptor for multiple PRRs, BAK1 is targeted by multiple pathogen effectors, as shown here and in previous reports (Macho and Zipfel, 2015). It is likely that plants have evolved to sense BAK1 perturbation by pathogen effectors (Tang and Zhou, 2016). Ectopic expression of an N-terminal truncated BAK1 leads to auto-immune responses in plants (Dominguez-Ferreras et al., 2015). The *bak1–4/bkk1* double mutant carrying loss-of-function mutations in *BAK1* and *SERK4* displays a strong hypersensitive response in the absence of pathogen infection (He et al., 2007). Recently, it was shown that genetic- or pathogen-induced depletion of BAK1 sensitizes immune signaling through PEPRs, which are PRRs that sense endogenous danger signal Peps (Yamada et al., 2016). Strikingly, HopB1 cleaves BAK1 only upon flg22 perception. The phosphorylation of BAK1 Thr455, which is known to stabilize the P loop for an active conformation (Yan et al., 2012), is also required for cleavage by HopB1. The stabilized P loop likely becomes accessible to HopB1, thereby ensuring that HopB1 attacks only when plant immunity is activated. This immune activation-dependent cleavage of BAK1 might have allowed HopB1 to dampen plant immunity with minimal perturbation to the host plant. Indeed, HopB1 does not trigger ETI when delivered from bacteria. Therefore, HopB1 activity reflects an adaptive strategy in the pathogen to avoid provoking host immunity.

EXPERIMENTAL PROCEDURES

Plant Materials, Constructs, and Primers

The plant materials and constructs used in this study are described in the Supplemental Experimental Procedures, and primers used are listed in Table S1.

Bacterial Growth Assays

For syringe infiltration, bacterial strains were collected and resuspended in water at 1×10^5 colony-forming units (CFU)/mL, then infiltrated into 4-week-old *Arabidopsis* leaves. Bacterial populations were determined at day 0 and day 3. For spray infection, bacteria were sprayed at 5×10^8 CFU/mL in water containing 0.02% Silwet L-77. The *Arabidopsis* leaves were kept under high humidity for 1 day, and bacterial populations were enumerated at 4 days post-inoculation.

ROS Production, *FRK1* Dual Reporter, and MAPK Phosphorylation Assay

ROS production assay was performed as described (Li et al., 2014). *FRK1* dual reporter and MAPK phosphorylation assays were carried out according to Feng et al. (2012).

His- and GST-Tagged Protein Purification

GST- and His-fusion recombinant proteins were expressed in *E.coli* and purified by affinity agarose beads as described by Li et al. (2014). Also see Supplemental Experimental Procedures.

GST Pull-Down and In Vitro Autophosphorylation Assays

GST pull-down assay was carried out as described (Li et al., 2014). For the in vitro phosphorylation assays, 1 μg of the indicated His-tagged proteins were loaded and detected using a pMIAGO-biotin phosphoprotein detection kit (Tymora) according to manufacturer's instruction.

CoIP Assay

CoIP assays were done as previously described (Li et al., 2014). Also see Supplemental Experimental Procedures.

Split-Luciferase Complementation Assay

Split-luciferase complementation assay was carried out as described (Chen et al., 2008). Also see Supplemental Experimental Procedures.

BAK1 Kinase Domain In Vitro Cleavage Assay

For the *E.coli* cleavage assays, GST-HopB1 or GST-HopB1 mutants were co-expressed with BAK1-His in *E.coli*. Bacterial cell cultures were treated with 0.4 mM IPTG at 20°C for 16 hr. The bacterial pellet was resuspended in a buffer containing 25 mM Tris-HCl (pH 7.5), 100 mM NaCl, and 1 mM DTT. Total proteins were extracted by adding SDS loading buffer and boiling at 100°C for 5 min and detected by anti-His and anti-GST (TianGen) immunoblots.

For in vitro cleavage assays, GST-HopB1 and BAK1KD-His recombinant proteins were purified, and 3 μg GST-HopB1 and 1 μg BAK1KD-His proteins were incubated in a tube at 25°C for 7 hr. The concentrations of indicated chemicals are as follows: AEBSF (0.1 mM, 1 mM), E-64 (10 μM, 100 μM), EDTA (0.1 mM, 1 mM), Pepstatin (10 μM, 100 μM), and PMSF (0.1 mM, 1 mM). The loaded proteins and cleavage product were detected by Coomassie brilliant blue staining and anti-His (TianGen) immunoblot.

Determination of Cleavage Sites by Mass Spectrometry

Protein bands on the SDS-PAGE gel were de-stained and reduced in 5% acetic anhydride for 1 hr and then in 10 mM DTT at 56°C for 30 min, followed by alkylation in 55 mM iodoacetamide in the dark for 1 hr. The protein bands were then in-gel digested with sequencing grade trypsin (10 ng/μL trypsin, 50 mM ammonium bicarbonate [pH 8.0]) overnight at 37°C. Peptides were extracted sequentially with 5% formic acid/50% acetonitrile and 0.1% formic acid/75% acetonitrile, then concentrated to ~20 μL. The extracted peptides were separated by an analytical capillary column (50 μm × 15 cm) packed with 5 μm spherical C18 reversed phase material (YMC). An Agilent nanoAcquity UPLC system (Agilent) was used to generate the following HPLC gradients: 0%–30% A in 40 min and 30%–70% B in 15 min (A = 0.1% formic acid in water; B = 0.1% formic acid in acetonitrile). The eluted peptides were sprayed into a LTQ mass spectrometer (ThermoFisher Scientific) equipped with a nano-ESI ion source. The mass spectrometer was operated in data-dependent mode with one MS scan followed by four CID (collision-induced dissociation) tandem MS scans for each cycle. Database searches were performed on an in-house Mascot server (Matrix Science Ltd.) against the BAK1 protein sequence. The search parameters were as follows: 7 ppm mass tolerance for precursor ions; 0.5 Da mass tolerance for product ions. Three missed cleavage sites were allowed for trypsin digestion, and the following variable modifications were included: oxidation on methionine, acetylation on protein N terminus and lysine, and carbamidomethylation on cysteine. The tandem MSs of matched acetylation on the protein N terminus were manually checked for their validity.

SUPPLEMENTAL INFORMATION

Supplemental Information includes Supplemental Experimental Procedures, five figures, and two tables and can be found with this article online at http://dx.doi.org/10.1016/j.chom.2016.09.007.

AUTHOR CONTRIBUTIONS

Conceptualization, L.L., S.C., and J.-M.Z.; Methodology, L.L., P.K., S.C., J.R.A., and J.-M.Z.; Investigation, L.L., P.K., L.Y., and G.C.; Resources, S.C., J.R.A., and J.-M.Z.; Writing – Original Draft, L.L. and J.-M.Z.; Writing – Review & Editing, P.K. and J.R.A.; Visualization, L.L. and P.K.; Supervision, J.R.A., S.C., and J.-M.Z.; Project Administration, J.-M.Z.; Funding Acquisition, J.R.A. and J.-M.Z.

ACKNOWLEDGMENTS

We thank Dr. Cyril Zipfel for sharing *bak1–5/bkk1* seeds. This work was funded by Chinese Natural Science Foundation (31320103909), the Chinese Ministry of Science and Technology grant 2015CB910200, the Strategic Priority Research Program of the Chinese Academy of Sciences (grant number XDB11020200), the Chinese Academy of Sciences international cooperation key project grant GJHZ1311, and the State Key Laboratory of Plant Genomics grant 2015B0129-02 to J.-M.Z., and the USA National Science Foundation grant 1508504 and funds from the Center for Plant Science Innovation at the University of Nebraska to J.R.A.

Received: March 16, 2016
Revised: July 30, 2016
Accepted: September 6, 2016
Published: October 12, 2016

REFERENCES

Albert, I., Böhm, H., Albert, M., Feiler, C.E., Imkampe, J., Wallmeroth, N., Brancato, C., Raaymakers, T.M., Oome, S., Zhang, H., et al. (2015). An RLP23-SOBIR1-BAK1 complex mediates NLP-triggered immunity. Nat Plants *1*, 15140.

Alfano, J.R., and Collmer, A. (2004). Type III secretion system effector proteins: double agents in bacterial disease and plant defense. Annu. Rev. Phytopathol. *42*, 385–414.

Axtell, M.J., Chisholm, S.T., Dahlbeck, D., and Staskawicz, B.J. (2003). Genetic and molecular evidence that the *Pseudomonas syringae* type III effector protein AvrRpt2 is a cysteine protease. Mol. Microbiol. *49*, 1537–1546.

Baird, T.T., Jr., Wright, W.D., and Craik, C.S. (2006). Conversion of trypsin to a functional threonine protease. Protein Sci. *15*, 1229–1238.

Boller, T., and Felix, G. (2009). A renaissance of elicitors: perception of microbe-associated molecular patterns and danger signals by pattern-recognition receptors. Annu. Rev. Plant Biol. *60*, 379–406.

Chen, H., Zou, Y., Shang, Y., Lin, H., Wang, Y., Cai, R., Tang, X., and Zhou, J.M. (2008). Firefly luciferase complementation imaging assay for protein-protein interactions in plants. Plant Physiol. *146*, 368–376.

Chinchilla, D., Zipfel, C., Robatzek, S., Kemmerling, B., Nürnberger, T., Jones, J.D., Felix, G., and Boller, T. (2007). A flagellin-induced complex of the receptor FLS2 and BAK1 initiates plant defence. Nature *448*, 497–500.

Cui, H., Tsuda, K., and Parker, J.E. (2015). Effector-triggered immunity: from pathogen perception to robust defense. Annu. Rev. Plant Biol. *66*, 487–511.

Cunnac, S., Chakravarthy, S., Kvitko, B.H., Russell, A.B., Martin, G.B., and Collmer, A. (2011). Genetic disassembly and combinatorial reassembly identify a minimal functional repertoire of type III effectors in *Pseudomonas syringae*. Proc. Natl. Acad. Sci. USA *108*, 2975–2980.

Dodds, P.N., and Rathjen, J.P. (2010). Plant immunity: towards an integrated view of plant-pathogen interactions. Nat. Rev. Genet. *11*, 539–548.

Dominguez-Ferreras, A., Kiss-Papp, M., Jehle, A.K., Felix, G., and Chinchilla, D. (2015). An overdose of the *Arabidopsis* coreceptor BAK1 or its ectodomain causes autoimmunity in a SOBIR1-dependent manner. Plant Physiol. *168*, 1106–1121.

Dou, D., and Zhou, J.M. (2012). Phytopathogen effectors subverting host immunity: different foes, similar battleground. Cell Host Microbe *12*, 484–495.

Feng, F., and Zhou, J.M. (2012). Plant-bacterial pathogen interactions mediated by type III effectors. Curr. Opin. Plant Biol. *15*, 469–476.

Feng, F., Yang, F., Rong, W., Wu, X., Zhang, J., Chen, S., He, C., and Zhou, J.M. (2012). A *Xanthomonas* uridine 5′-monophosphate transferase inhibits plant immune kinases. Nature *485*, 114–118.

Fu, Z.Q., Guo, M., Jeong, B.R., Tian, F., Elthon, T.E., Cerny, R.L., Staiger, D., and Alfano, J.R. (2007). A type III effector ADP-ribosylates RNA-binding proteins and quells plant immunity. Nature *447*, 284–288.

Gimenez-Ibanez, S., Hann, D.R., Ntoukakis, V., Petutschnig, E., Lipka, V., and Rathjen, J.P. (2009). AvrPtoB targets the LysM receptor kinase CERK1 to promote bacterial virulence on plants. Curr. Biol. *19*, 423–429.

Göhre, V., Spallek, T., Häweker, H., Mersmann, S., Mentzel, T., Boller, T., de Torres, M., Mansfield, J.W., and Robatzek, S. (2008). Plant pattern-recognition receptor FLS2 is directed for degradation by the bacterial ubiquitin ligase AvrPtoB. Curr. Biol. *18*, 1824–1832.

He, P., Shan, L., Lin, N.C., Martin, G.B., Kemmerling, B., Nürnberger, T., and Sheen, J. (2006). Specific bacterial suppressors of MAMP signaling upstream of MAPKKK in *Arabidopsis* innate immunity. Cell *125*, 563–575.

He, K., Gou, X., Yuan, T., Lin, H., Asami, T., Yoshida, S., Russell, S.D., and Li, J. (2007). BAK1 and BKK1 regulate brassinosteroid-dependent growth and brassinosteroid-independent cell-death pathways. Curr. Biol. *17*, 1109–1115.

Hedstrom, L. (2002). Serine protease mechanism and specificity. Chem. Rev. *102*, 4501–4524.

Heese, A., Hann, D.R., Gimenez-Ibanez, S., Jones, A.M., He, K., Li, J., Schroeder, J.I., Peck, S.C., and Rathjen, J.P. (2007). The receptor-like kinase SERK3/BAK1 is a central regulator of innate immunity in plants. Proc. Natl. Acad. Sci. USA *104*, 12217–12222.

Hotson, A., Chosed, R., Shu, H., Orth, K., and Mudgett, M.B. (2003). *Xanthomonas* type III effector XopD targets SUMO-conjugated proteins *in planta*. Mol. Microbiol. *50*, 377–389.

Jones, J.D., and Dangl, J.L. (2006). The plant immune system. Nature *444*, 323–329.

Kadota, Y., Sklenar, J., Derbyshire, P., Stransfeld, L., Asai, S., Ntoukakis, V., Jones, J.D., Shirasu, K., Menke, F., Jones, A., and Zipfel, C. (2014). Direct regulation of the NADPH oxidase RBOHD by the PRR-associated kinase BIK1 during plant immunity. Mol. Cell *54*, 43–55.

Kazan, K., and Lyons, R. (2014). Intervention of phytohormone pathways by pathogen effectors. Plant Cell *26*, 2285–2309.

Khan, M., Subramaniam, R., and Desveaux, D. (2016). Of guards, decoys, baits and traps: pathogen perception in plants by type III effector sensors. Curr. Opin. Microbiol. *29*, 49–55.

Kim, J.G., Stork, W., and Mudgett, M.B. (2013). *Xanthomonas* type III effector XopD desumoylates tomato transcription factor SlERF4 to suppress ethylene responses and promote pathogen growth. Cell Host Microbe *13*, 143–154.

Kvitko, B.H., Park, D.H., Velásquez, A.C., Wei, C.F., Russell, A.B., Martin, G.B., Schneider, D.J., and Collmer, A. (2009). Deletions in the repertoire of *Pseudomonas syringae* pv. *tomato* DC3000 type III secretion effector genes reveal functional overlap among effectors. PLoS Pathog. *5*, e1000388.

Le Roux, C., Huet, G., Jauneau, A., Camborde, L., Trémousaygue, D., Kraut, A., Zhou, B., Levaillant, M., Adachi, H., Yoshioka, H., et al. (2015). A receptor pair with an integrated decoy converts pathogen disabling of transcription factors to immunity. Cell *161*, 1074–1088.

Li, X., Lin, H., Zhang, W., Zou, Y., Zhang, J., Tang, X., and Zhou, J.M. (2005). Flagellin induces innate immunity in nonhost interactions that is suppressed by *Pseudomonas syringae* effectors. Proc. Natl. Acad. Sci. USA *102*, 12990–12995.

Li, L., Li, M., Yu, L., Zhou, Z., Liang, X., Liu, Z., Cai, G., Gao, L., Zhang, X., Wang, Y., et al. (2014). The FLS2-associated kinase BIK1 directly phosphorylates the NADPH oxidase RbohD to control plant immunity. Cell Host Microbe *15*, 329–338.

Lozano-Durán, R., Bourdais, G., He, S.Y., and Robatzek, S. (2014). The bacterial effector HopM1 suppresses PAMP-triggered oxidative burst and stomatal immunity. New Phytol. *202*, 259–269.

Lu, D., Wu, S., Gao, X., Zhang, Y., Shan, L., and He, P. (2010). A receptor-like cytoplasmic kinase, BIK1, associates with a flagellin receptor complex to initiate plant innate immunity. Proc. Natl. Acad. Sci. USA *107*, 496–501.

Macho, A.P., and Zipfel, C. (2014). Plant PRRs and the activation of innate immune signaling. Mol. Cell *54*, 263–272.

Macho, A.P., and Zipfel, C. (2015). Targeting of plant pattern recognition receptor-triggered immunity by bacterial type-III secretion system effectors. Curr. Opin. Microbiol. *23*, 14–22.

Macho, A.P., Schwessinger, B., Ntoukakis, V., Brutus, A., Segonzac, C., Roy, S., Kadota, Y., Oh, M.H., Sklenar, J., Derbyshire, P., et al. (2014). A bacterial tyrosine phosphatase inhibits plant pattern recognition receptor activation. Science *343*, 1509–1512.

Narayanan, A., and Jones, L.H. (2015). Sulfonyl fluorides as privileged warheads in chemical biology. Chem. Sci. *6*, 2650–2659.

Nicaise, V., Joe, A., Jeong, B.R., Korneli, C., Boutrot, F., Westedt, I., Staiger, D., Alfano, J.R., and Zipfel, C. (2013). *Pseudomonas* HopU1 modulates plant immune receptor levels by blocking the interaction of their mRNAs with GRP7. EMBO J. *32*, 701–712.

Nomura, K., Debroy, S., Lee, Y.H., Pumplin, N., Jones, J., and He, S.Y. (2006). A bacterial virulence protein suppresses host innate immunity to cause plant disease. Science *313*, 220–223.

Ntoukakis, V., Saur, I.M., Conlan, B., and Rathjen, J.P. (2014). The changing of the guard: the Pto/Prf receptor complex of tomato and pathogen recognition. Curr. Opin. Plant Biol. *20*, 69–74.

Powers, J.C., Asgian, J.L., Ekici, O.D., and James, K.E. (2002). Irreversible inhibitors of serine, cysteine, and threonine proteases. Chem. Rev. *102*, 4639–4750.

Rawlings, N.D., and Barrett, A.J. (2013). Introduction: serine peptidases and their clans. In Hand of Proteolytic Enzymes, Third Edition (Academic Press), pp. 2491–2523.

Rawlings, N.D., Waller, M., Barrett, A.J., and Bateman, A. (2014). MEROPS: the database of proteolytic enzymes, their substrates and inhibitors. Nucleic Acids Res. *42*, D503–D509.

Roux, M., Schwessinger, B., Albrecht, C., Chinchilla, D., Jones, A., Holton, N., Malinovsky, F.G., Tör, M., de Vries, S., and Zipfel, C. (2011). The *Arabidopsis* leucine-rich repeat receptor-like kinases BAK1/SERK3 and BKK1/SERK4 are required for innate immunity to hemibiotrophic and biotrophic pathogens. Plant Cell *23*, 2440–2455.

Sarris, P.F., Duxbury, Z., Huh, S.U., Ma, Y., Segonzac, C., Sklenar, J., Derbyshire, P., Cevik, V., Rallapalli, G., Saucet, S.B., et al. (2015). A plant immune receptor detects pathogen effectors that target WRKY transcription factors. Cell *161*, 1089–1100.

Schwessinger, B., Roux, M., Kadota, Y., Ntoukakis, V., Sklenar, J., Jones, A., and Zipfel, C. (2011). Phosphorylation-dependent differential regulation of plant growth, cell death, and innate immunity by the regulatory receptor-like kinase BAK1. PLoS Genet. *7*, e1002046.

Shao, F., Merritt, P.M., Bao, Z., Innes, R.W., and Dixon, J.E. (2002). A *Yersinia* effector and a *Pseudomonas* avirulence protein define a family of cysteine proteases functioning in bacterial pathogenesis. Cell *109*, 575–588.

Shao, F., Golstein, C., Ade, J., Stoutemyer, M., Dixon, J.E., and Innes, R.W. (2003). Cleavage of *Arabidopsis* PBS1 by a bacterial type III effector. Science *301*, 1230–1233.

Söding, J., Biegert, A., and Lupas, A.N. (2005). The HHpred interactive server for protein homology detection and structure prediction. Nucleic Acids Res. *33*, W244-8.

Spoel, S.H., and Dong, X. (2012). How do plants achieve immunity? Defence without specialized immune cells. Nat. Rev. Immunol. *12*, 89–100.

Sun, Y., Li, L., Macho, A.P., Han, Z., Hu, Z., Zipfel, C., Zhou, J.M., and Chai, J. (2013). Structural basis for flg22-induced activation of the *Arabidopsis* FLS2-BAK1 immune complex. Science *342*, 624–628.

Tang, D., and Zhou, J.M. (2016). PEPRs spice up plant immunity. EMBO J. *35*, 4–5.

Wang, X., Kota, U., He, K., Blackburn, K., Li, J., Goshe, M.B., Huber, S.C., and Clouse, S.D. (2008). Sequential transphosphorylation of the BRI1/BAK1 receptor kinase complex impacts early events in brassinosteroid signaling. Dev. Cell *15*, 220–235.

Wang, Y., Li, J., Hou, S., Wang, X., Li, Y., Ren, D., Chen, S., Tang, X., and Zhou, J.M. (2010). A *Pseudomonas syringae* ADP-ribosyltransferase inhibits *Arabidopsis* mitogen-activated protein kinase kinases. Plant Cell *22*, 2033–2044.

Wang, G., Roux, B., Feng, F., Guy, E., Li, L., Li, N., Zhang, X., Lautier, M., Jardinaud, M.F., Chabannes, M., et al. (2015). The decoy substrate of a pathogen effector and a pseudokinase specify pathogen-induced modified-self recognition and immunity in plants. Cell Host Microbe *18*, 285–295.

Xiang, T., Zong, N., Zou, Y., Wu, Y., Zhang, J., Xing, W., Li, Y., Tang, X., Zhu, L., Chai, J., and Zhou, J.M. (2008). *Pseudomonas syringae* effector AvrPto blocks innate immunity by targeting receptor kinases. Curr. Biol. *18*, 74–80.

Xin, X.F., and He, S.Y. (2013). *Pseudomonas syringae* pv. *tomato* DC3000: a model pathogen for probing disease susceptibility and hormone signaling in plants. Annu. Rev. Phytopathol. *51*, 473–498.

Xu, H., Shan, J., Jurukovski, V., Yuan, L., Li, J., and Tian, K. (2007). *TSP50* encodes a testis-specific protease and is negatively regulated by *p53*. Cancer Res. *67*, 1239–1245.

Yamada, K., Yamashita-Yamada, M., Hirase, T., Fujiwara, T., Tsuda, K., Hiruma, K., and Saijo, Y. (2016). Danger peptide receptor signaling in plants ensures basal immunity upon pathogen-induced depletion of BAK1. EMBO J. *35*, 46–61.

Yan, L., Ma, Y., Liu, D., Wei, X., Sun, Y., Chen, X., Zhao, H., Zhou, J., Wang, Z., Shui, W., and Lou, Z. (2012). Structural basis for the impact of phosphorylation on the activation of plant receptor-like kinase BAK1. Cell Res. *22*, 1304–1308.

Zhang, J., Shao, F., Li, Y., Cui, H., Chen, L., Li, H., Zou, Y., Long, C., Lan, L., Chai, J., et al. (2007). A *Pseudomonas syringae* effector inactivates MAPKs to suppress PAMP-induced immunity in plants. Cell Host Microbe *1*, 175–185.

Zhang, J., Li, W., Xiang, T., Liu, Z., Laluk, K., Ding, X., Zou, Y., Gao, M., Zhang, X., Chen, S., et al. (2010). Receptor-like cytoplasmic kinases integrate signaling from multiple plant immune receptors and are targeted by a *Pseudomonas syringae* effector. Cell Host Microbe *7*, 290–301.

Zhang, W., Fraiture, M., Kolb, D., Löffelhardt, B., Desaki, Y., Boutrot, F.F., Tör, M., Zipfel, C., Gust, A.A., and Brunner, F. (2013). Arabidopsis receptor-like protein30 and receptor-like kinase suppressor of BIR1-1/EVERSHED mediate innate immunity to necrotrophic fungi. Plant Cell *25*, 4227–4241.

Zhou, J.M., and Chai, J. (2008). Plant pathogenic bacterial type III effectors subdue host responses. Curr. Opin. Microbiol. *11*, 179–185.